NiAl–TiC–Al_2O_3 composite formed by self-propagation high-temperature synthesis process: combustion behaviour, microstructure, and properties

Tri Widodo Besar Riyadi[a], Tao Zhang[b], Denis Marchant[b], Xiaomeng Zhu[c]

a. Faculty of Engineering, Universitas Muhammadiyah Surakarta, Jl. A. Yani Tromol Pos 1 Pabelan Kartasura Surakarta, Jawa Tengah 57102, Indonesia
b. Faculty of Science, Engineering and Computing, Kingston University, London SW15 3DW, UK
c. School of Materials Science and Engineering, Wuhan University of Technology, PR China

* Corresponding author. Tel.: +62 271 717417 ext 3292

E-mail addresses: Tri.Riyadi@ums.ac.id

Abstract

Intermetallic-ceramic composites formed by the self-propagation high-temperature synthesis (SHS) process have attracted much interest in research development since they offer low-cost production and mechanical properties that have characteristically high performance. The objective of this work was to study the effect of reactant compositions on the combustion behaviour, microstructure and mechanical properties of the synthesized product of NiAl–TiC–Al_2O_3 composite. The reaction mechanism of the synthesized products was discussed based on the observations of the combustion reaction and the microstructure characterization. The results provided information on the relationship between the reactant composition, microstructure and the properties of the products of NiAl–TiC–Al_2O_3 composites formed by the SHS process.

Keywords: NiAl–TiC–Al_2O_3 composite, reactant compositions, self-propagation high-temperature synthesis, combustion behaviour

1. Introduction

NiAl has been attractive as a potential candidate for high-temperature applications due to its advantages such as high strength, low density, high melting temperature, and good oxidation and corrosion resistance [1]. However, the application of single phase NiAl for structural materials is still limited due to its lack of ductility at room temperature and insufficient strength at high temperature. Inspired by the strengthening of master alloy [2], many efforts have been made to balance NiAl properties such as using grain refinement to improve its ductility at room temperature, and alloying or compositing for strengthening when used in high-temperature applications.

Several studies for compositing NiAl were carried out using the addition of ceramics such as carbide [3], boride [4], nitride [5], and oxide [6], or a single metal [7]. A study for strengthening NiAl–Al_2O_3 composites by grain refinement was carried out using mechano-synthesis in ball milling. The crystal structure of synthesized NiAl and Al_2O_3 was measured in nanometer size of around 11–19 nm after 10 hours milling time, and 8 nm after being milled for 60 hours [8]. TiB_2–NiAl composites were synthesized by arch melting to study the strengthening effect of TiB_2 dispersion in the NiAl matrix. Introduction of the rare earth element Ce resulted in the refined grain size of TiB_2 [9]. An investigation on TiC–TiB–NiAl composites reveals that the grain size of the synthesized products was reduced by increasing the NiAl content [10]. A study on TiB_2–Al_2O_3–NiAl composites synthesized by the SHS process indicates that the higher content of TiB_2–Al_2O_3 produced more regular shapes and homogenous distributions of TiB_2–Al_2O_3 particles in the NiAl matrix [11]. A study to improve

the tensile properties of NiAl at room and high temperature was conducted by alloying using the strengthening mechanism for the Fe–Ni–Al–Cr heat resistant steels with the addition of Mo. It was reported that the tensile properties and deformation of NiAl at room temperatures were strongly dependent on the precipitate of NiAl. The alloy with optimum Mo content can exhibit high strength at high temperature until 923 K [7]. NiAl/WC composites were produced by thermal explosion reactions to study the tribological properties of the system at high temperature. The results showed that the lowest friction coefficient and wear rate can be achieved by adding 30 wt.% WC [12]. The fabrications of ceramic composites of NiAl reinforced by TiB_2/TiC and TiB_2/TiN using the SHS process were conducted by C.L. Yeah et al. Decreasing the NiAl from 70 to 40 mol% in the composite systems, the fracture toughness of the composite with TiB_2/TiC additions was improved from 4.2 to 5.8 MPa $m^{1/2}$, and in the range of 3.86–5.5 MPa $m^{1/2}$ for the composite with TiB_2 and TiN reinforcements [13]. TiC/Ni_3(Al,Ti)–NiAl composites were synthesized by reactive hot pressing. TiC grains adhered well to the Ni_3(Al,Ti)–NiAl alloys because Ti_3AlC_2 materials tend to be out-diffused. The composites exhibit superior mechanical properties at 1500 ˚C because of the elimination of pores. Flexural strength and fracture toughness at room temperature and high temperature were measured, and reached the greatest values at 800 ˚C [14].

Among the ceramic materials, TiC has attracted much interest as a reinforcement candidate for NiAl since it offers great advantages such as high hardness, high melting temperature, and high corrosion and wear resistance [15]. It has been reported that the combination of high hardness and excellent stability of TiC at high temperature, together with the strong atomic bonds of NiAl produces composites with an excellent wear resistance at room and high temperature [3]. An alumina ceramic system with TiC–Al_2O_3 has been reported to improve the fracture toughness of individual ceramic materials, either TiC or Al_2O_3 [16]. L.Y.

Sheng et al. [17] fabricated NiAl–TiC composite with dispersed Al_2O_3 oxides to form NiAl–TiC–Al_2O_3 composite using the SHS process and hot extrusion technique. It was reported that NiAl–TiC–Al_2O_3 composite possess better mechanical properties at room temperature due to a fine microstructure and pre-deformation caused by the hot extrusion.

During the last six decades, the SHS process has attracted a special interest to synthesize refractory and hard materials such as intermetallic, ceramic and composite. When compared with conventional methods, the SHS process has many advantages such as a shorter processing time and a lower energy consumption [18]. In an SHS process, the reactant powders are compacted and subsequently ignited to initiate the combustion processin a high exothermic reaction. The heat released by the reaction of the front layer then propagates and heats up the adjacent layers to the ignition temperature of the SHS process until a part or the whole reactant is transformed into product. The ignition of the SHS process has also developed using many different techniques, with non-contact methods such as laser and microwave [19]. Recent studies showed that induction heating offers significant advantages as a clean and efficient external heat source for use in combustion synthesis, owing to its rapid heating characteristics. Induction heating was successfully used to ignite the combustion synthesis of NiAl/Al_2O_3[6] and NiAl/TiC [3].

Although the SHS process offers significant advantages for the synthesis of NiAl and NiAl based composites, the high porosity of the synthesized products is still problematic [20]. The material synthesized using the SHS process is often associated with a high level of porosity, which can lead to only 50% of the theoretical density being achieved [21]. The application of a porous product affects the oxidation resistance of coatings and therefore cannot be tolerated since it can permit the infiltration of gas from outside to the base metal to create an oxidation reaction. The porosity, however, is beneficial for some applications

such as biomaterials [22], ceramic foams [23], and a large number of filtration applications [24]. Understanding the pore structure and its formation in synthesized product therefore becomes one of the main challenges to produce a desirable product. It is worth mentioning that the research on the SHS process of NiAl–TiC–Al_2O_3 composite using induction heating was very limited. L.Y. Sheng et al. [17] conducted the investigation of NiAl–TiC–Al_2O_3 composite from Ni, Al, Ti, C and TiO_2 using the SHS process with hot extrusion, where the punch used to extrude the reactant was heated using induction heating. However, the combustion temperature of the SHS process was not monitored due to the limitations of the experimental set up. It has been realised that a study of the combustion behaviour could provide direct information to understand the reaction mechanism, which will help to control the microstructure and improve the mechanical properties of the synthesized product [6].

The objective of this work was to fabricate NiAl–TiC–Al_2O_3 composite using Ni, Al, C and TiO_2 as the raw materials, by using the SHS process and induction heating as the ignition source. The research was focused on investigating the effect of reactant compositions on the combustion behaviour, microstructure, and mechanical properties of the synthesized products. In this work, TiO_2 were used to produce TiC since it is a low cost material and has relatively high surface area to mass ratio owing to its fine particle size, compared to Ti powder [25]. The method used to produce PAN-based CNF by Wu et al. reported in Ref. [26] may be used as competitor to produce TiC as reported by Ref. [27]. However, this technique does not offer the advantage of the SHS process described in the present work which is able to promote the development of the optimum structure of the NiAl–TiC–Al_2O_3 composites with less energy requirement.

2. Material and methods

The powders used for the reactants in the SHS process were Ni carbonyl type–123 (4.5 μm, 99.85%), Al (45 μm, 99.7%), and C (1 μm, 99.9%) supplied by William Rowland UK. The TiO_2 (0.3 μm, 93–96%) used in this investigation was manufactured by Huntsman Tioxide UK. The SEM micrographs of reactant powders are shown in Fig. 1. The reactants were prepared by mixing two stoichiometric compositions of (1-x)(Ni + Al) and x($3TiO_2$ + 4Al + 3C), where x is 0, 10, 20, 30 and 40 wt.%. The composition of reactant was determined since the reactions were expected to occur according to Eq. (1) and Eq. (2).

$$Ni + Al \rightarrow NiAl \quad (1)$$

$$3TiO_2 + 4Al + 3C \rightarrow 3TiC + 2Al_2O_3 \quad (2)$$

The starting materials were dry mixed using a ceramic mortar for approximately 30 minutes and dried in a carbolite furnace at about 100 °C for 1 hour to remove any moisture contents. The powder mixture was weighed to produce 2 grams for each reactant and subsequently cold compacted using a pressure of 200 MPa to form a pellet with a size of 16 mm in diameter. The resulting height of the pellet after compaction was approximately 3.3 mm. The SHS processes of the reactants were performed inside a glove box with an atmosphere of argon with a gas flow rate of 15 l/min and a pressure of 13.8 MPa. Induction heating was used to initiate the combustion reaction using an electric current of 300 A for all processes, which is the highest available current of the equipment and provided the fastest heating rate. When the SHS process started, the induction heating was turned off after approximately 1 second. The ignition of the SHS process can be seen from the white glow of the burnt sample accompanied by a sudden increase of the combustion temperature. The combustion temperature was measured using a pyrometer with a temperature range of 540–3000 °C and a response time of 2 ms. The data were recorded using a computer equipped with Raytek DataTemp Multidrop software. The emissivity of all samples was assumed to be

0.82, which is similar to the emissivity of NiAl as the major content in the mixture. The accuracy of the measurement at the temperature below 1100 ^{o}C was calibrated with a type K thermocouple. A scanning electron microscope equipped with EDX analysis was used to observe the microstructure of the synthesized products, while the phase identification was carried out using XRD operated at 40 kV/200 mA with a scanning step of 0.02 deg and a scanning rate of 4 deg./min. Prior to the SEM and XRD tests, the samples were polished and etched using a standard procedure as mentioned in Ref. [28]. The mechanical property of the synthesized products was evaluated using a Vickers microhardness indentation under a load of 0.1 N for 15 seconds.

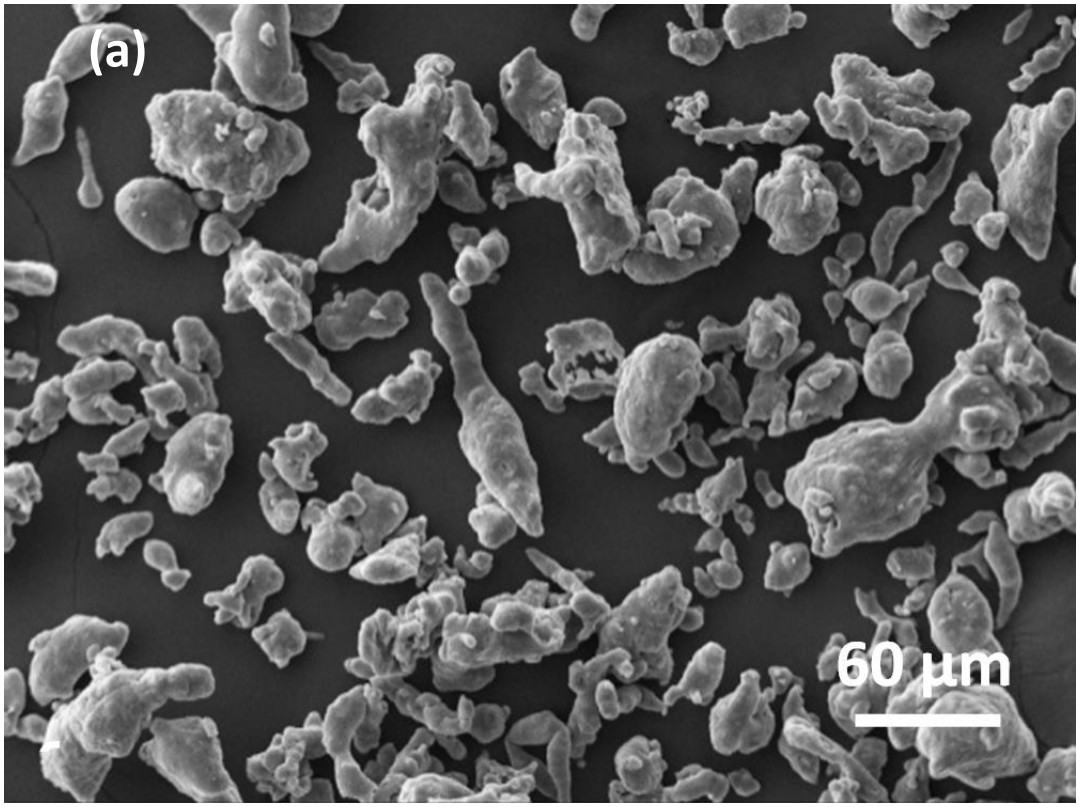

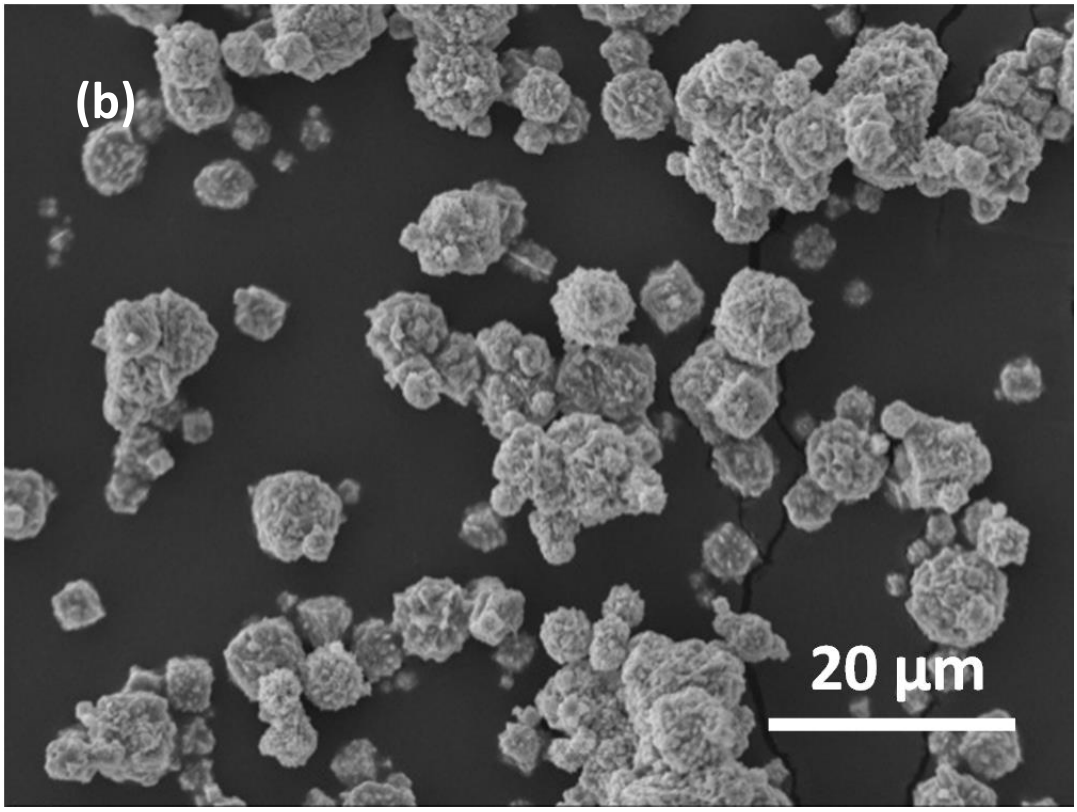
(b)
20 µm

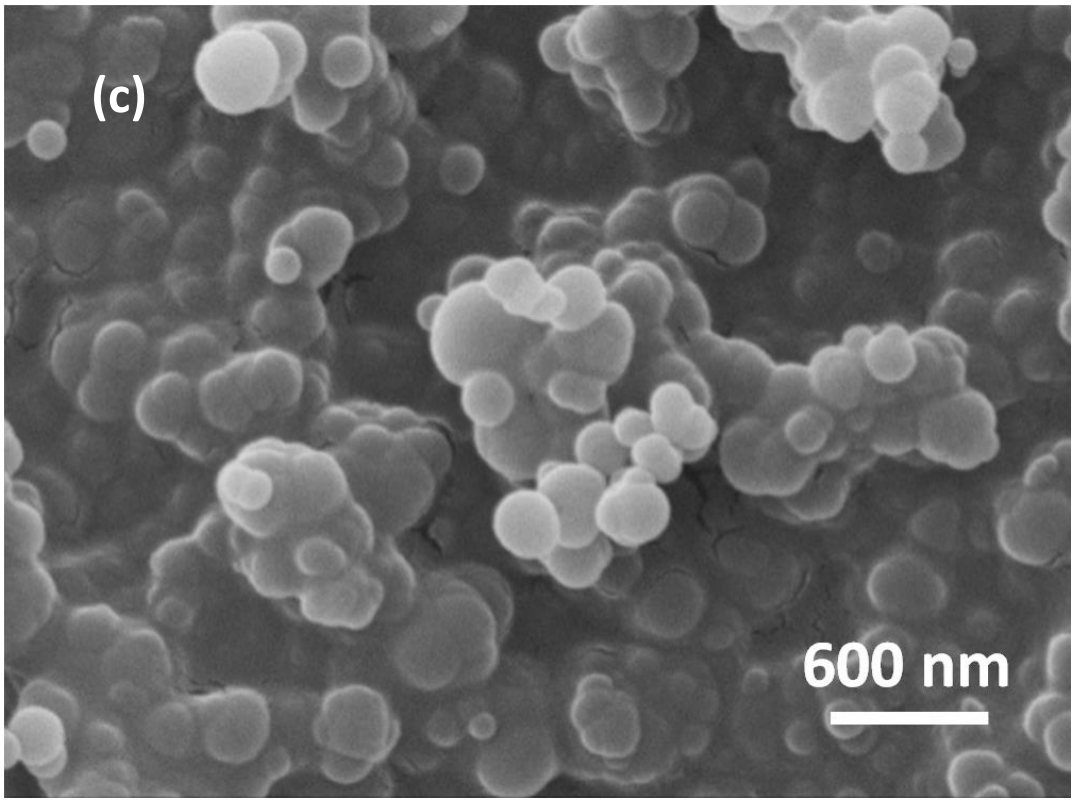
(c)
600 nm

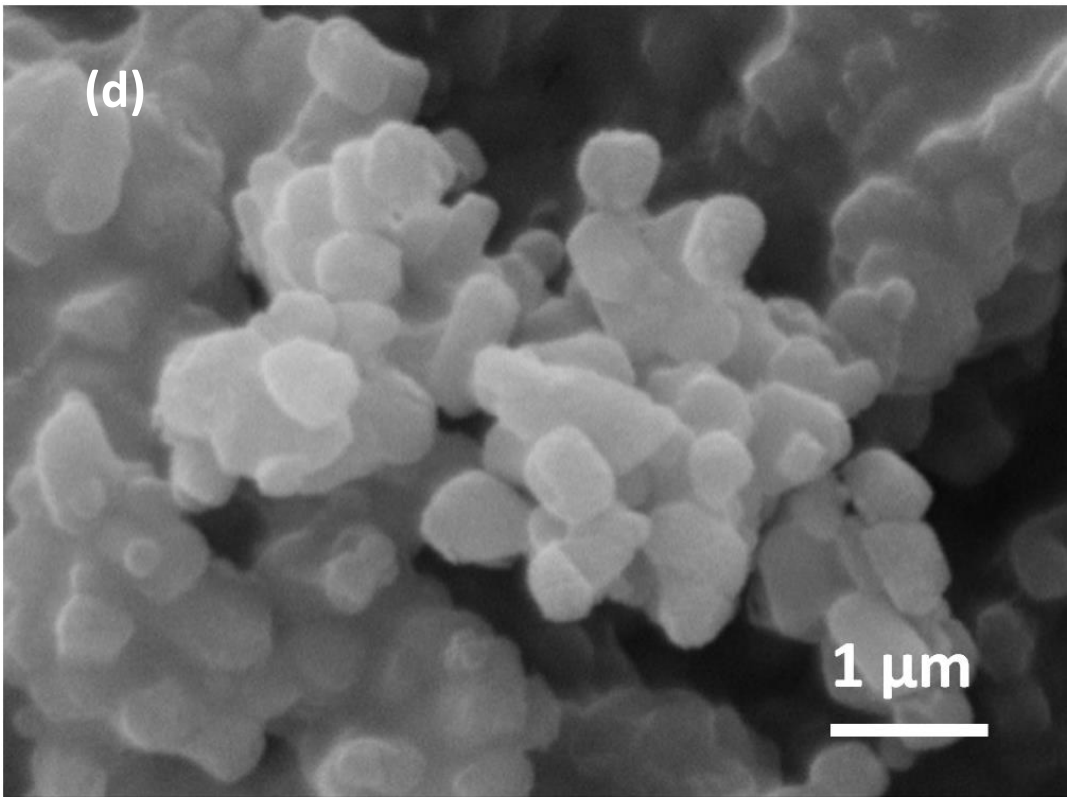

Fig. 1 Back Scattered Electron (BSE) images of reactant powders: (a) Al; (b) Ni; (c) C; and (d) TiO_2

3. Results

3.1. Phases of the synthesized products

Fig. 2(a–e) show the XRD patterns of the synthesized products prepared by (1–x)Ni/Al + (x)3TiO_2/4Al/3C with x = 0, 10, 20, 30 and 40 wt.%, respectively. It can be observed in all samples that no XRD peaks of the original reactants can be found indicating that the SHS processes were completed. In Fig. 2(a), the XRD peaks confirm that the reaction product is pure NiAl. In Fig. 2(b-e), the phase compositions of the synthesized products mainly contain the composite systems of NiAl, TiC, and Al_2O_3, except Fig. 2(d) which includes the appearance of Ni_5Al_3 phase. In Fig. 2(b, c, and e), there are only three phases in the synthesized products which consist of NiAl, TiC, and Al_2O_3. This demonstrates that the initial reactants have been transformed thoroughly to the expected products. In Fig. 2(d), a small amount of Ni_5Al_3 phase

was found in the final product. According to the phase diagram of Ni–Al system [20], the formation of intermediate phase Ni_5Al_3 can be formed during cooling below ~700 °C.

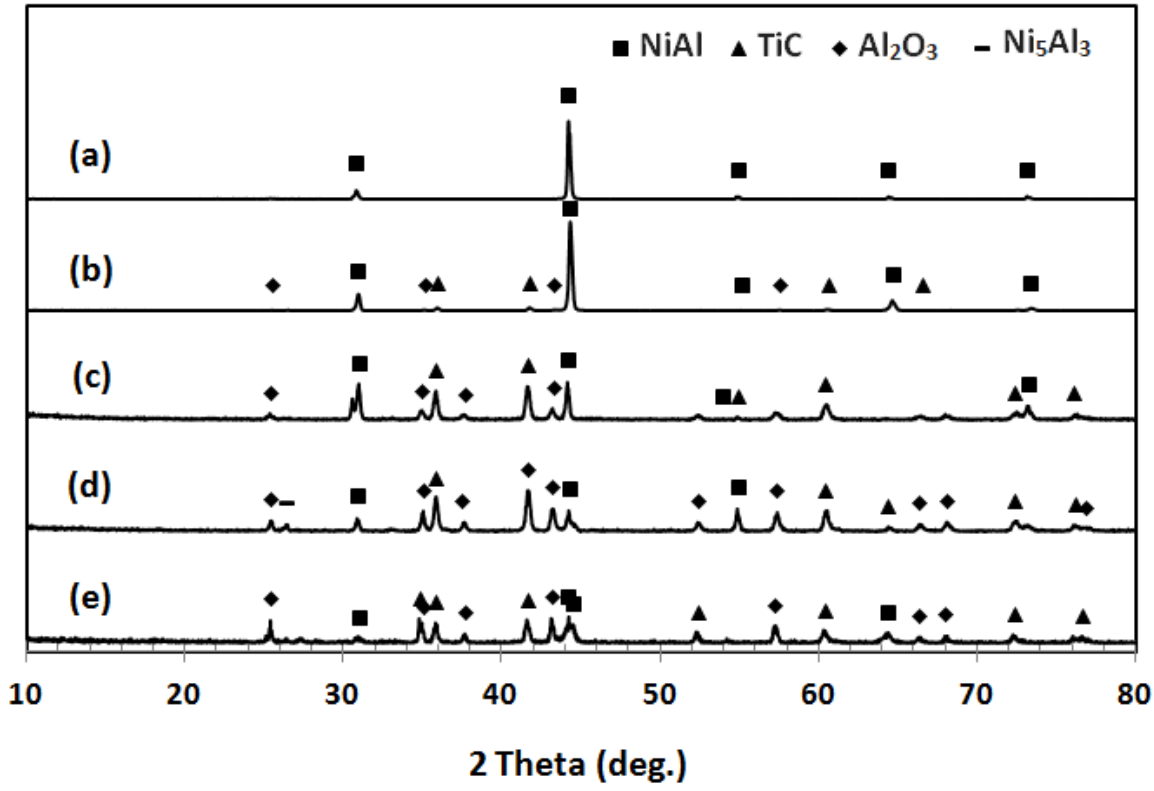

Fig. 2 X-rays diffraction patterns of the synthesized products prepared by (1-x)(Ni/Al) + x($3TiO_2$/4Al/3C) with x: (a) 0; (b) 10; (c) 20; (d) 30; and (e) 40 wt.%

3.2. Combustion temperature

Fig. 3 shows the temperature profiles for the SHS reactions of the samples which are composed of (1–x)Ni/Al + (x)$3TiO_2$/4Al/3C with x equals to 10, 20, 30, and 40 wt.%. Since the temperature measurement was only recorded using a pyrometer, the combustion temperature could only be monitored starting from 813 K (540 °C) which is the lowest value of the temperature range of the pyrometer. As can be seen in Fig. 3, all the samples produce a temperature profile with a similar trend showing a typical combustion temperature of the SHS process which consists of initial heating, combustion, and solidification [3][6][28]. The

ignition temperature, maximum combustion temperature and plateau are shown in Fig. 3. The first stage showing a peak temperature of the combustion zone may be attributed to the exothermic reactions ofNi/Al followed by TiC–Al_2O_3, and the second stage showing a plateau may correspond to the solidification of NiAl. This assumption was taken based on the reason that, in the first stage, Ni/Al was synthesized first and the heat released by the NiAl was subsequently used to ignite the reaction of TiO_2/Al/C to form TiC–Al_2O_3 resulting in a simultaneous temperature increase. The high combustion temperature of the TiO_2/Al/C reaction then maintained the melting of the NiAl for a period of time before cooling down rapidly after full solidification. As reported by Zhu et al. [29] and Rahbari et al. [30] that the ignition temperature of the SHS reaction of NiAl and TiO_2/Al/C are 833 K and 1144 K, respectively.

The effect of reactant compositions on the combustion behaviour, particularly the ignition temperature, maximum combustion temperature and the length of the plateau observed in Fig. 3 is given in Table 1. The ignition temperatures are increased with an increase of the TiO_2/Al/C content. The ignition temperature of the samples with compositions of 0, 10, 20, 30, and 40 wt.% of TiO_2/Al/C can be identified at approximately 813.3 K, 852.6 K, 1005.3 K, 1039.6 K, and 1133.4 K, respectively. This indicates that the ignition can occur at a temperature below the melting point of Al (933 K), as the lowest melting point in the system. It is worth mentioning that in most SHS processes for NiAl, the reaction is initiated by the melting of Al which subsequently spreads into the solid element to produce ignition [31]. However, it is possible for a lower ignition temperature to occur, as reported by Makino et al. [32] which showed that the ignition of NiAl can be 200 K lower than the melting point of Al depending on the size ratio and the mixture ratio. They reported that the reduction of the ignition temperature can be achieved by increasing the particle surface area of the reactant.

As noted from literary sources, Ignition occurs if the heat released by a reaction is greater than that lost to the atmosphere [15][20]. The increase of the ignition temperature caused by increasing the content of TiO_2/Al/C may be explained as follows: (1) Increasing the content of TiO_2/Al/C will absorb more heat released by the NiAl reaction which results in the increase of the heat required to initiate the exothermic reaction of the system (2) increasing the content of TiO_2/Al/C will reduce the thermal conductivity of the sample due to the addition of low thermal conductivity material TiO_2, and results in a slower reaction rate of Ni/Al and (3) increasing the content of TiO_2/Al/C will reduce the contact between Ni and Al.

As expected, an increase in the TiO_2/Al/C content increased the maximum temperature of the combustion process. In this investigation, the maximum combustion temperature is referred to as the maximum point in the combustion temperature profiles, which is shown in Fig. 3. As given in Table 1, the maximum combustion temperatures of the first reaction for the samples with 0, 10, 20, 30 and 40 wt.% of TiO_2/Al/C are approximately 1900 K, 1911 K, 2093 K, 2135 K, and 2208 K, respectively. This result suggests that the maximum combustion temperature for all reactions are below the melting point of TiC (3210 K) [33] and Al_2O_3 (2325 K) [34]. The increase in the combustion temperature can be attributed to the increase of the amount of TiO_2/Al/C particles since the reaction to produce TiC–$Al_2O_3$from TiO_2/Al/C is more exothermic. An increase in the TiO_2/Al/C content, however, can reduce the thermal conductivity of the reactant which can reduce the degree of completion of the SHS reaction, lengthen the ignition time, or even stop the initiation of the reaction. As can be seen in Fig. 3, the ignition time is significantly longer with an increase in the TiO_2/Al/C content. This is because a lower percentage of TiO_2/Al/C content had a higher content of the liquid NiAl in the synthesized product which, in-turn, increased the thermal conductivity of the reactant. Consequently, the higher thermal conductivity of the reactants improved the speed of the

reaction. Where the content ofTiO_2/Al/C is higher, the ignition time is longer due to the lower thermal conductivity. In the sample with 10 wt.% of TiO_2/Al/C, the maximum combustion temperature is approximately 1911 K, which is the same as the adiabatic temperature or the maximum temperature in the SHS process of Ni/Al. The re-melting of the reaction product NiAl will absorb the heat released by the TiO_2/Al/C reaction. As a consequence, the combustion temperature was reduced. It can be observed that the subsequent increase in the content of TiO_2/Al/C from 10 to 40 wt.% significantly increases the maximum combustion temperature from 1911K to 2208 K. The reason for this may be explained by the fact that when the content of TiO_2/Al/C in the preforms is increased, the heat released by the exothermic reactions of TiO_2/Al/C per unit volume of the preforms is also increased.

It can be observed that increasing the TiO_2/Al/C content reduces the duration of the plateau owing to the reduction in content of the low melting product, NiAl. It can also be seen that the temperature of the plateau for the different reactant compositions is almost the same at about 1890 K, which corresponds to the solidification temperature of NiAl. The small variance from the melting temperature of NiAl at 1911 K may be due to measurement error.

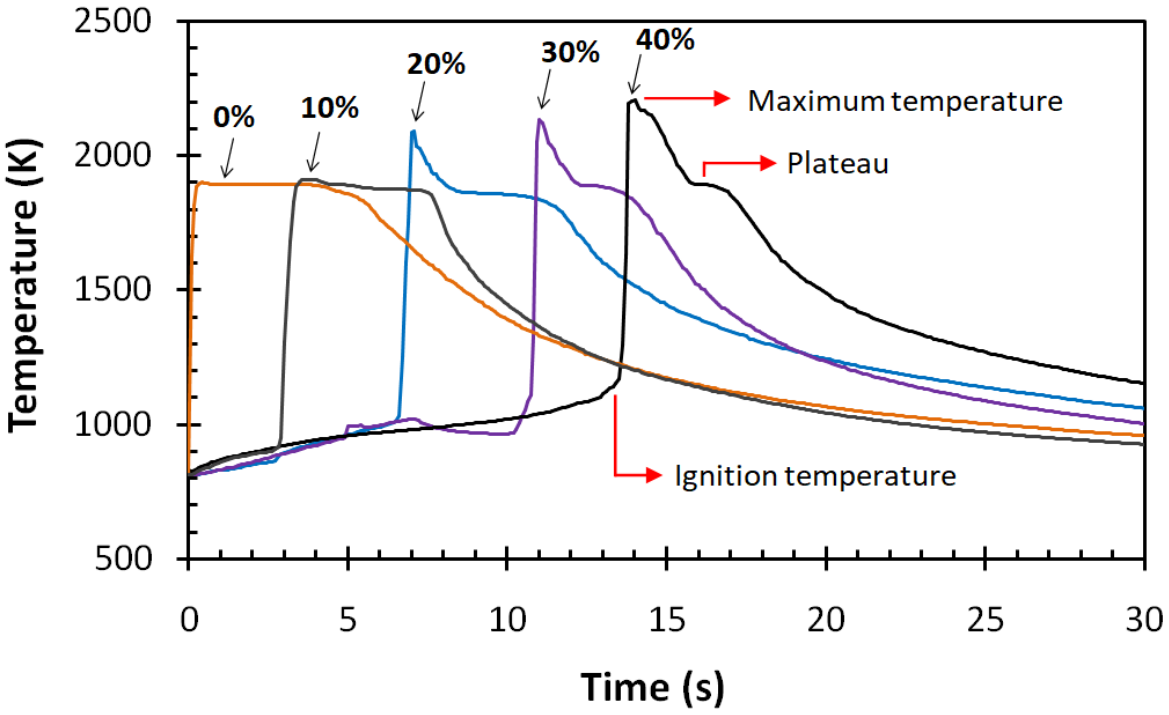

Fig. 3 Temperature profiles of the SHS process of Ni/Al with 10, 20, 30, and 40 wt.% TiO_2/Al/C

Table 1 Data of combustion temperature profile

	Weight percentage (wt.%) of TiO_2/Al/C				
	0	**10**	**20**	**30**	**40**
Ignition temperature (K)	813.1	852.6	1005.3	1039.6	1133.4
Maximum temperature (K)	1900	1911	2093	2135	2208
Duration of plateau (s)	4.59	3.2	2.9	1.7	0.85

3.3. Microstructure

In order to verify the existence of the phases in the synthesized products as observed by XRD, the microstructural distribution of the phases was characterized by SEM techniques. Fig. 4(a-e) shows the typical back scattered electron (BSE) images of the synthesized products

prepared by (1-x)Ni/Al + x($3TiO_2$/4Al/3C) with x = 0, 10, 20, 30 and 40 wt.%, respectively. In Fig. 4(a), the microstructure of synthesized product prepared using pure Ni/Al shows a bright and homogeneous structure. In Fig. 4(b–e), the microstructure of the synthesized products prepared by x = 10, 20, 30 and 40 wt.% TiO_2/Al/C, respectively, shows that the synthesized products are comprised of bright areas, dark particles, and grey zones. To provide more detailed information about the shape and size of the phases, the enlarged images of the microstructures of the synthesized products with 10 and 30 wt.% of TiO_2/Al/C, respectively are shown in Fig. 4(b) and (d). The element compositions of the bright, dark and grey areas as described in Fig. 4(b) were further characterized using an EDX technique at positions of A, B, and C. The normalized data for the atomic compositions of the elementsis given in Table 2. The element compositions in the spot A show that the bright area is composed of Ni and Al with a weight percentage of 71.37 and 30.92, respectively. Quantification on the atomic fraction indicates that the atomic percentage of Ni and Al points to a composition of 50.93 and 47.99, respectively. This result is nearly close to an atomic ratio of 1 and 1, which confirms that the bright phase is NiAl. The element compositions in the spot B show that the dark particle is mainly composed of 62.36 wt.% Ti. In the theoretical calculation of the weight percentage, the weight fraction of Ti and C in the stoichiometric TiC is 79.94 and 20.06, respectively. It is apparent that the difference of Ti content between the results obtained by calculation and through observation is significantly large, which can be attributed to the presence of Ni and Al. This is because the resolution of the electron beam, which is 5 μm x 5 μm x 5 μm, could not precisely detect the element composition in the particle marked by the spot B, which has a grain size of approximately 1-2μm (shown in Fig. 4(b)). By referring to the XRD results in Fig. 2, it is likely that a high content of Ti at spot B indicates the phase of TiC. The high magnification figure showing the shape and average grain size of a TiC particle (1

μm) given in Fig. 4(b) is very consistent with the previous result as reported by Zhu et al. [3] who synthesized NiAl–TiC using induction heating, and other works [14][10]. However, the TiC in Ref. [3] was obtained using Ti and C as the reactants, while the result from the present study reveals that TiC can be synthesized with TiO_2/Al/C. This therefore suggests that TiC can be produced using low-cost material (TiO_2). The formation of TiC with a fine grain size can be attributed to the fast cooling during synthesis since there is insufficient time for the formed crystals to grow [35]. The weight fraction of the spot C indicates that the grey area represents a high content of Al and O. The atomic fraction of Al and O is 34.85 and 64.99, respectively. By referring to the XRD in Fig. 2, the spot C indicates the formation of Al_2O_3.

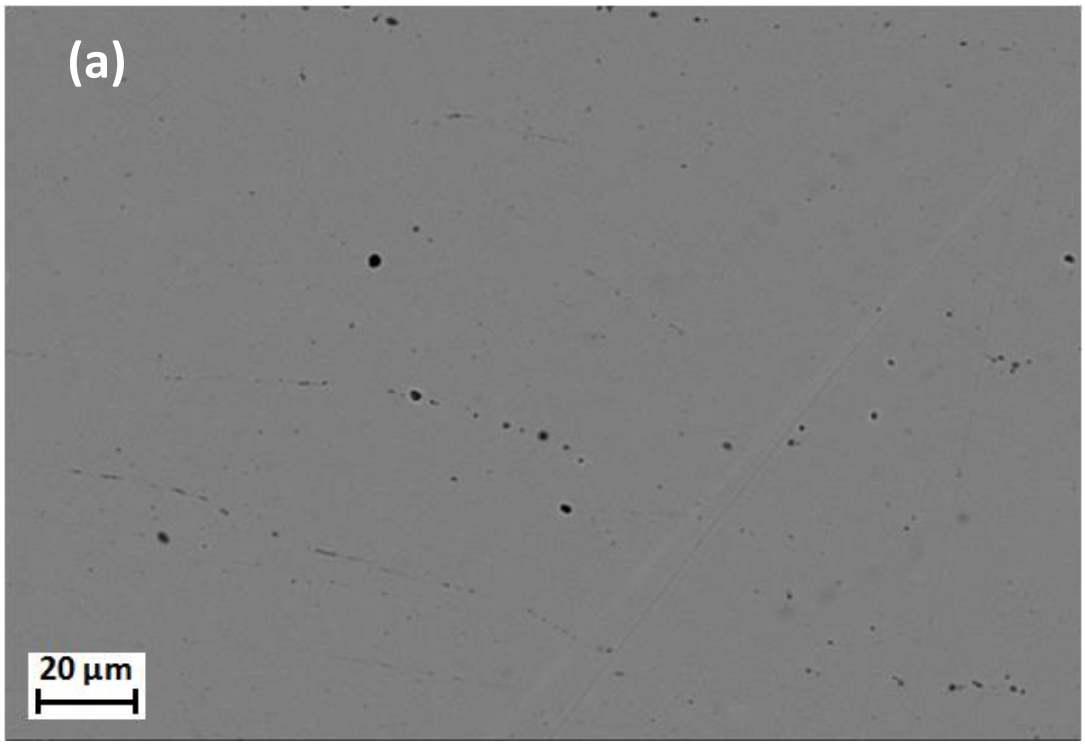

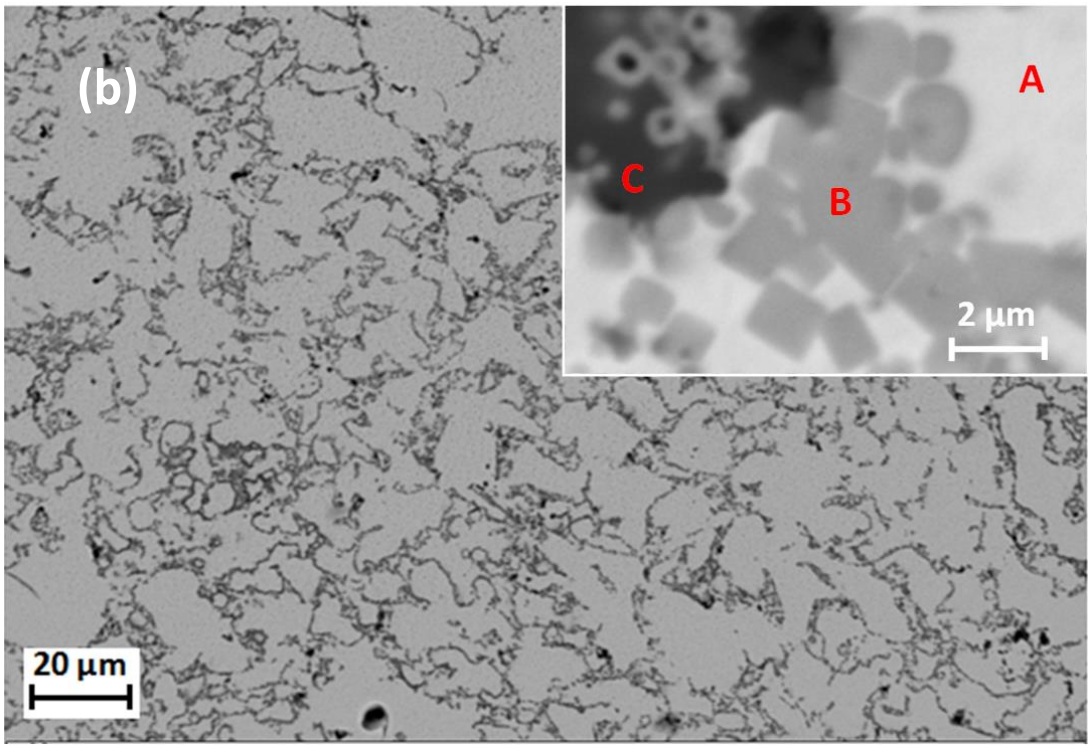
(b)
A
C
B
2 µm
20 µm

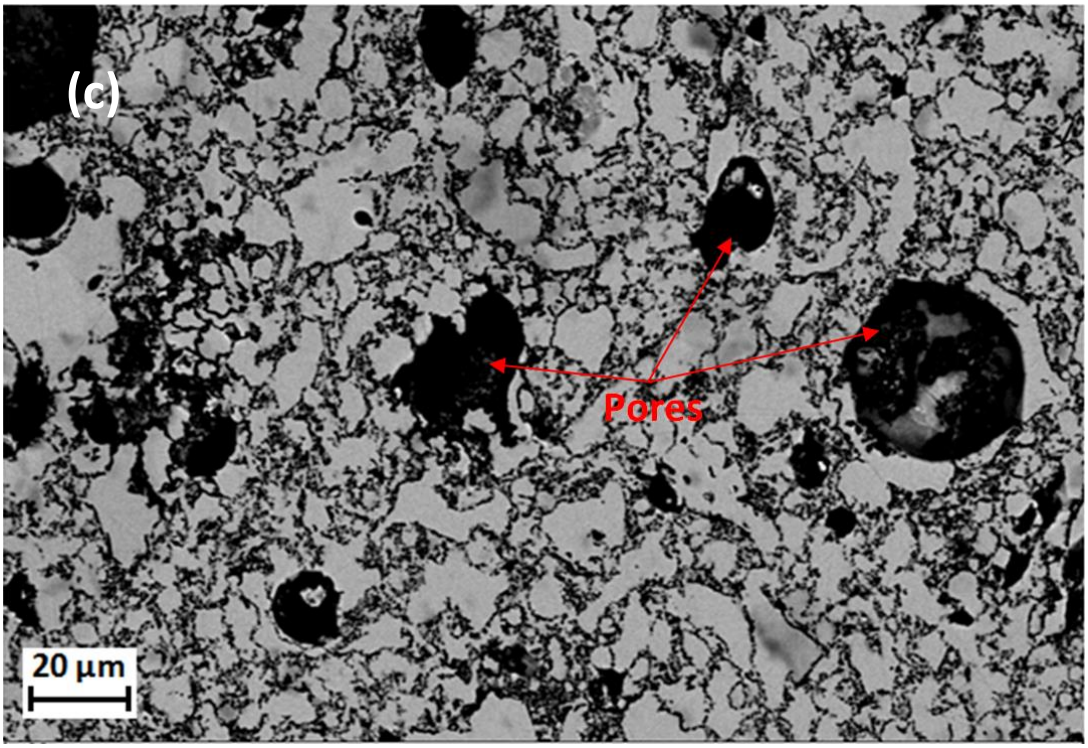
(c)
Pores
20 µm

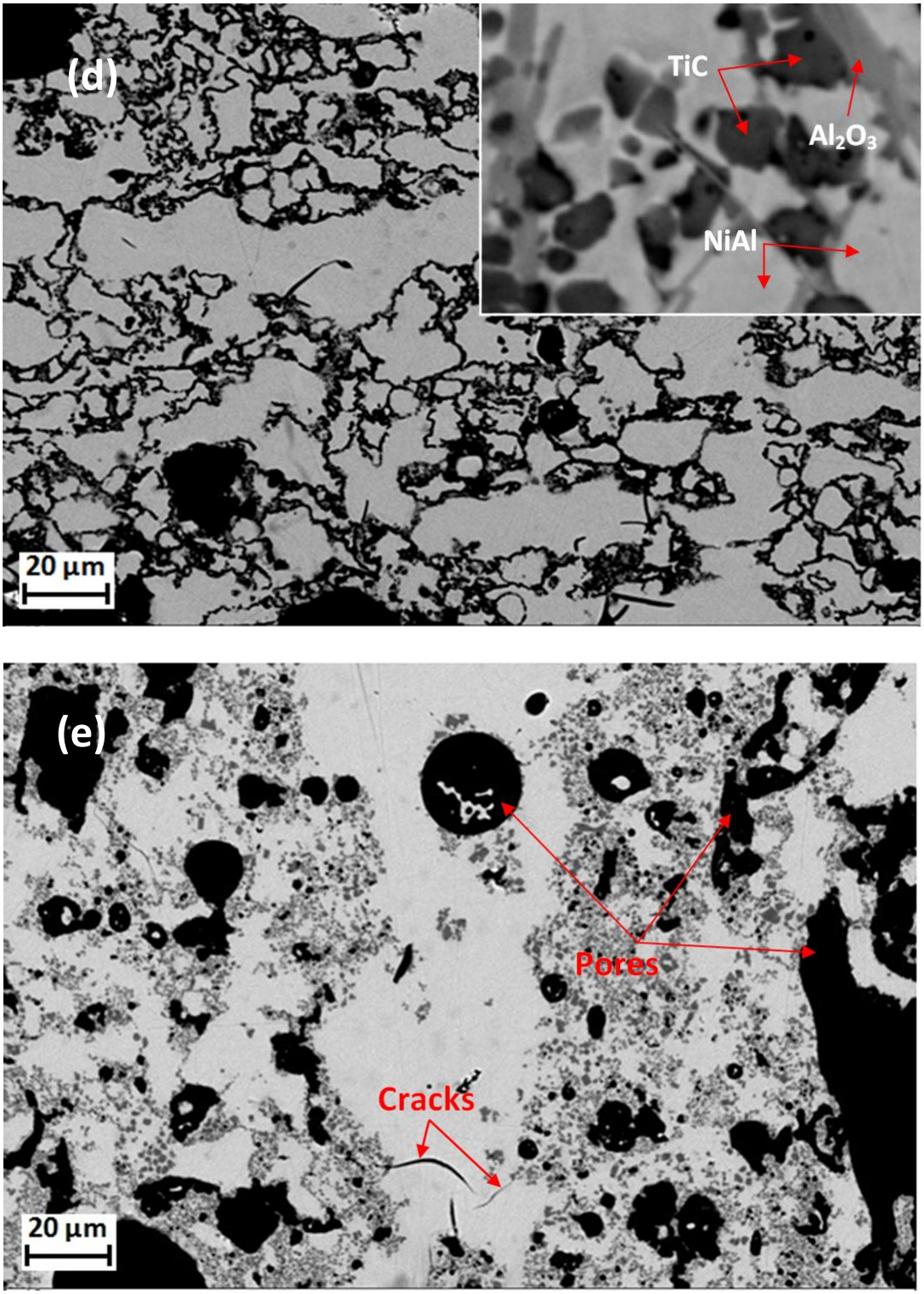

Fig. 4 Back Scattered Electron (BSE) images of NiAl–TiC–Al_2O_3 composites prepared by Ni/Al with: (a) 0; (b) 10; (c) 20; (d) 30; and (e) 40 wt.% of TiO_2/Al/C

Table 2 Chemical compositions in at.% of the spot A, B and C in Fig. 4(b)

Spectrum	O	Ne	Al	P	Ti	Ni	Total
A			47.99	0.49	0.59	50.93	100
B		5.117	11.53		70.30	13.05	100
C	64.99		34.85			0.15	100

The SEM micrographs shown in Fig. 4(b-e) reveal that the synthesized product is a composite with NiAl phase as the matrix and fine TiC particles as the dispersed phase. However, the distribution of TiC particles is inhomogeneous and concentrated along the NiAl grain boundary, which is in line with the results reported in Ref. [36]. In addition, Zhu et al. [3] who investigated the combustion synthesis of NiAl–TiC prepared from elemental powders showed that a high concentration of TiC appeared at the NiAl grain boundary illustrating that NiAl is synthesized before TiC is formed. Further synthesis of TiC then melts the NiAl causing some TiC to be embedded in the NiAl. In the case where there is a higher content of ceramic addition, as shown in Fig. 4(b-e), TiC and Al_2O_3 particles prefer to be segregated in the shell of pores. This result is consistent with that obtained by L.Y. Sheng et al. [17] who investigated the SHS process of NiAl–TiC–Al_2O_3 composite using hot extrusion. They reported that TiC and Al_2O_3 particles mostly appeared in the surface of the cavity formed after the SHS reaction. Comparing the product microstructures in Fig. 4(b) and (d), it can be seen that the morphology of the phases is significantly affected by the TiO_2/Al/C content. An increase of the TiO_2/Al/C content from 10 to 30 wt.% changes the shape and size of the TiC particles. The shape of the TiC particles changes from rectangular/hexagonal/tetrahedron to spherical, in addition, the size of the TiC particles is increased from about 1-2 micron to 2-3 micron. The increase of TiC size can be attributed to its nucleation and growth after reaction since TiC has a higher melting temperature than that of NiAl and Al_2O_3. This finding is in close agreement with previous work

done by Hu [14]. In this work, however, the increase of the TiO_2/Al/C contents also affects the shape of Al_2O_3 altering it from a cluster to a more distributed shape in the form of a line along the NiAl matrix, which can be attributed to the self-diffusion of Al_2O_3 [11]. In particular, the existence of liquid NiAl allows the Al_2O_3 to rise to the surface due to its lower density [35].

It can also be seen in Fig. 4(a) that the microstructure of the pure NiAl is significantly dense. An increase in the content of TiC–Al_2O_3 in the composite system, as shown in Fig. 4(b–e), increases the porosity of the synthesized products. The highest density of the composites can be found in the sample with 10 wt.% TiO_2/Al/C. This result suggests that the presence of a large amount of intermetallic phase NiAl in the composites can be used to improve the density of the product. Increasing the content of TiO_2/Al/C from 20 to 40 wt.% increased the porosity of the synthesized products. A higher fraction of pores can be found in the higher ceramic content. The reason for the increased porosity with an increase in the TiC–Al_2O_3 content can be related to the temperature profile as shown in Fig. 3. It was shown that the maximum combustion temperature for all reactions is above the melting point of NiAl and below the melting point of TiC and Al_2O_3. This result indicates that the formed NiAl was in the liquid state, while the TiC and Al_2O_3 formed during the reaction were in a solid state. Therefore, an increase in the TiC and Al_2O_3 content increases the presence of solid phases and reduces the liquid content during the synthesis process in the composite resulting in a higher porosity in the final products. As shown in Fig. 3, the amount of NiAl content was linked with the length of the plateau in the profile of the combustion temperature. Considering that a higher amount of NiAl could generate denser products, the existence of NiAl therefore not only became the ignition agent for the SHS reaction of TiC–Al_2O_3 systems, but also served as the diluents and binder. Besides pores, microcracks were also observed in the sample with a high TiC–Al_2O_3 content. The formation of cracks in the composite system produced by the SHS

process can be attributed to the intrinsic stress generated by the mismatch of thermal expansion coefficients between the different phases during cooling [37].

3.4. Mechanical properties

The microhardness of the synthesized products prepared by Ni/Al with various compositions of TiO_2/Al/C is shown in Fig. 5. The addition of TiC–Al_2O_3 content on the NiAl increases the hardness of the synthesized products. It is clearly shown in Fig. 5 that the increase in microhardness of the synthesized products is proportional to the addition of TiO_2/Al/C (the synthesis of TiC and Al_2O_3). A liniear equation to describe the increase of the hardness (HV) as a function of the weight fraction of TiO_2/Al/C (x) may be displayed as HV = 7.43x + 337, with 0.95 confidence level. The microstructure and phase analysis shown in sections 3.1-3.3 suggest that an increase in the product microhardness can be attributed to the higher volume fraction of TiC and Al_2O_3 particles in the products. Fig. 6(a-e) shows the typical photo micrograph of the Vickers indentation test conducted on the synthesized product with 0, 10, 20, 30 and 40 wt.% TiO_2/Al/C. Following examination of the indentation in the sample no crack was observed, even when the indentation was made at the area with a high concentration of ceramic particles. This indicates that a considerable improvement in the hardness of synthesized products containing a high content of ceramic particles can be achieved, without a reduction to their toughness.

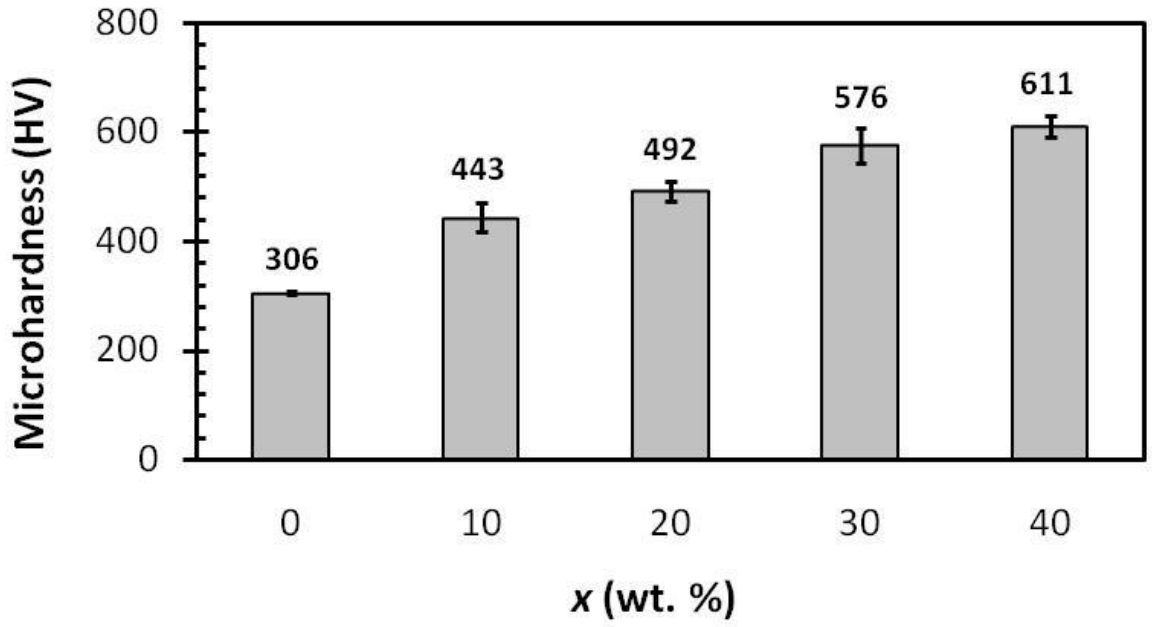

Fig. 5 Microhardness of synthesized products prepared by (1-x)Ni/Al + x(TiO_2/Al/C) with x = 0, 10, 20, 30 and 40 wt. %

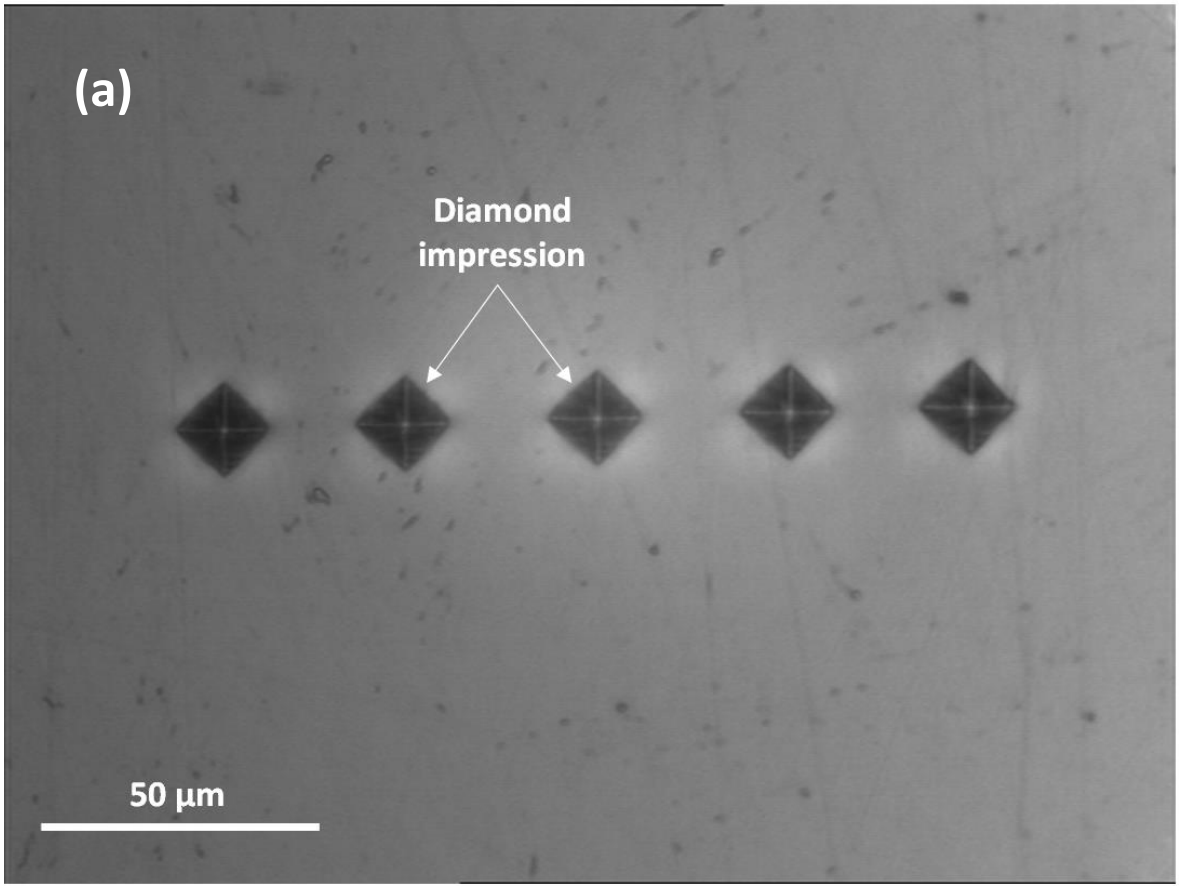

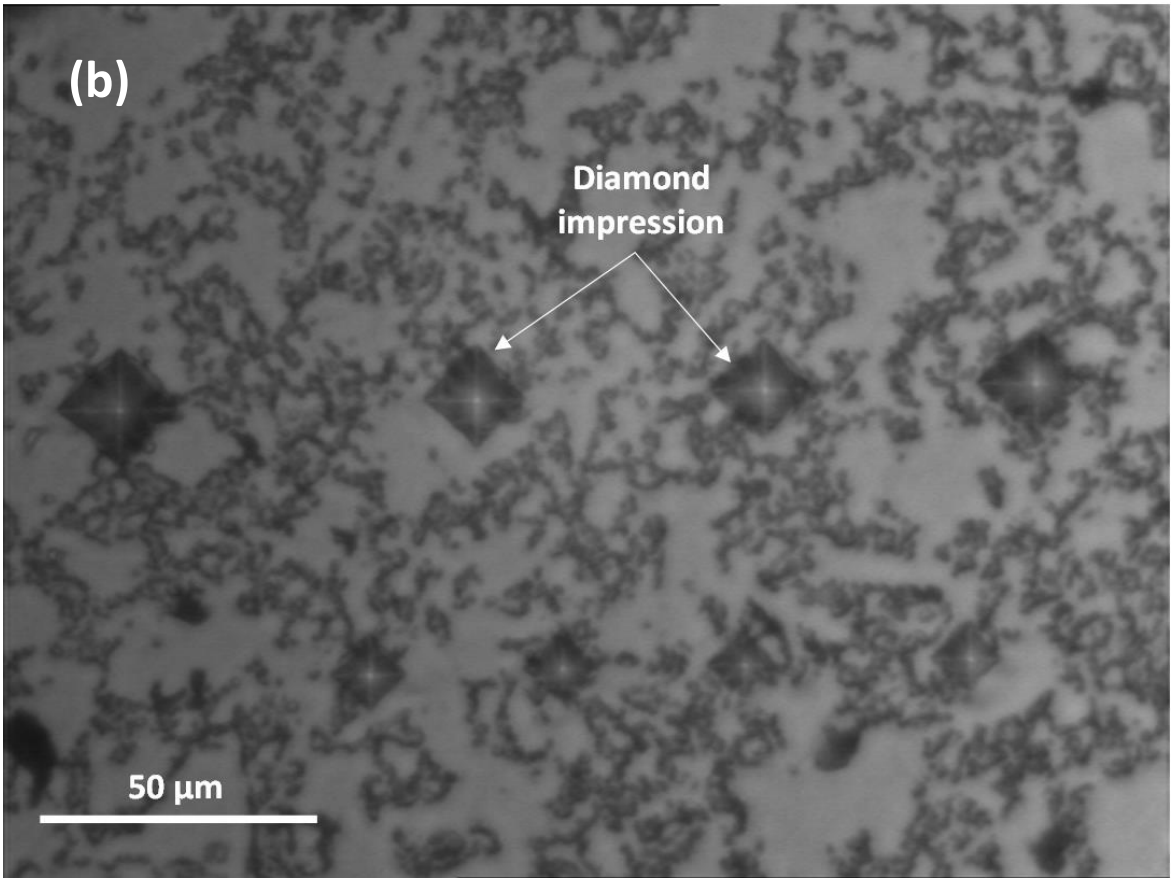
(b)
Diamond
impression
50 µm

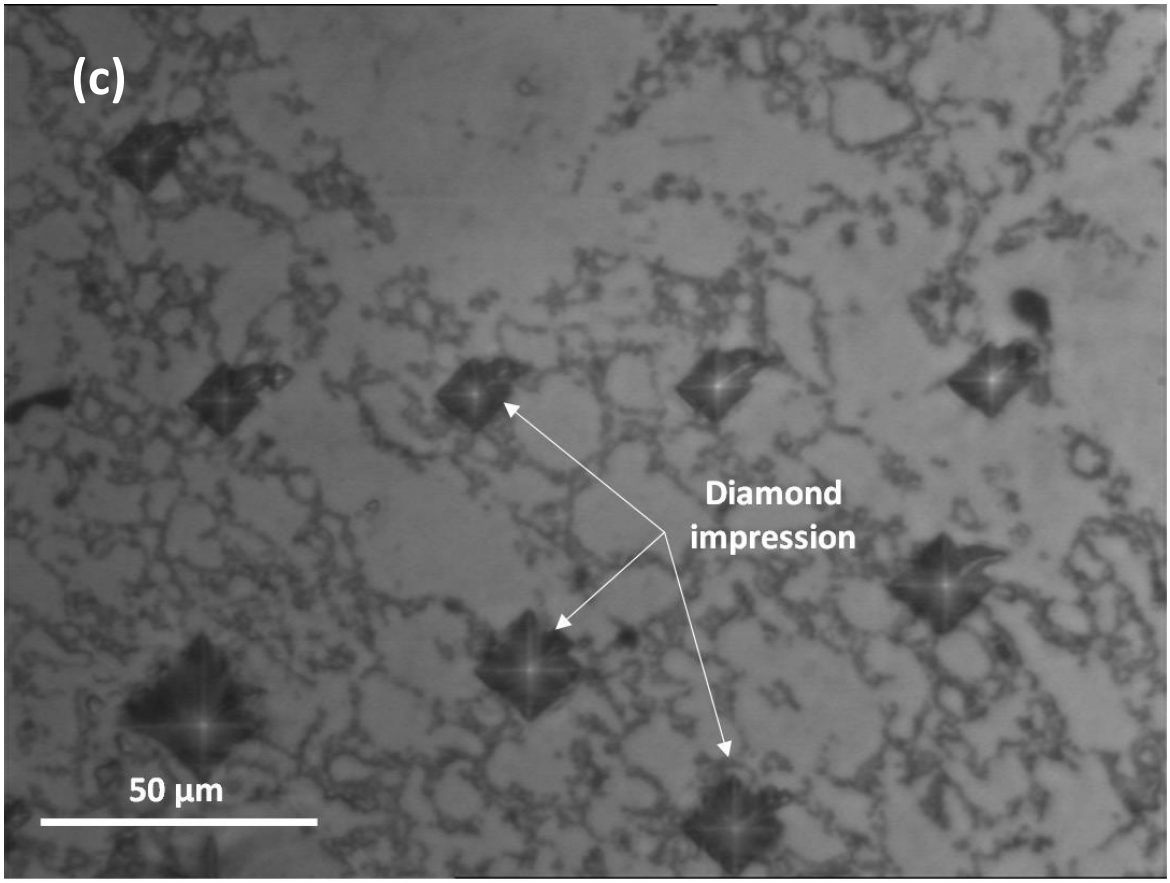
(c)
Diamond
impression
50 µm

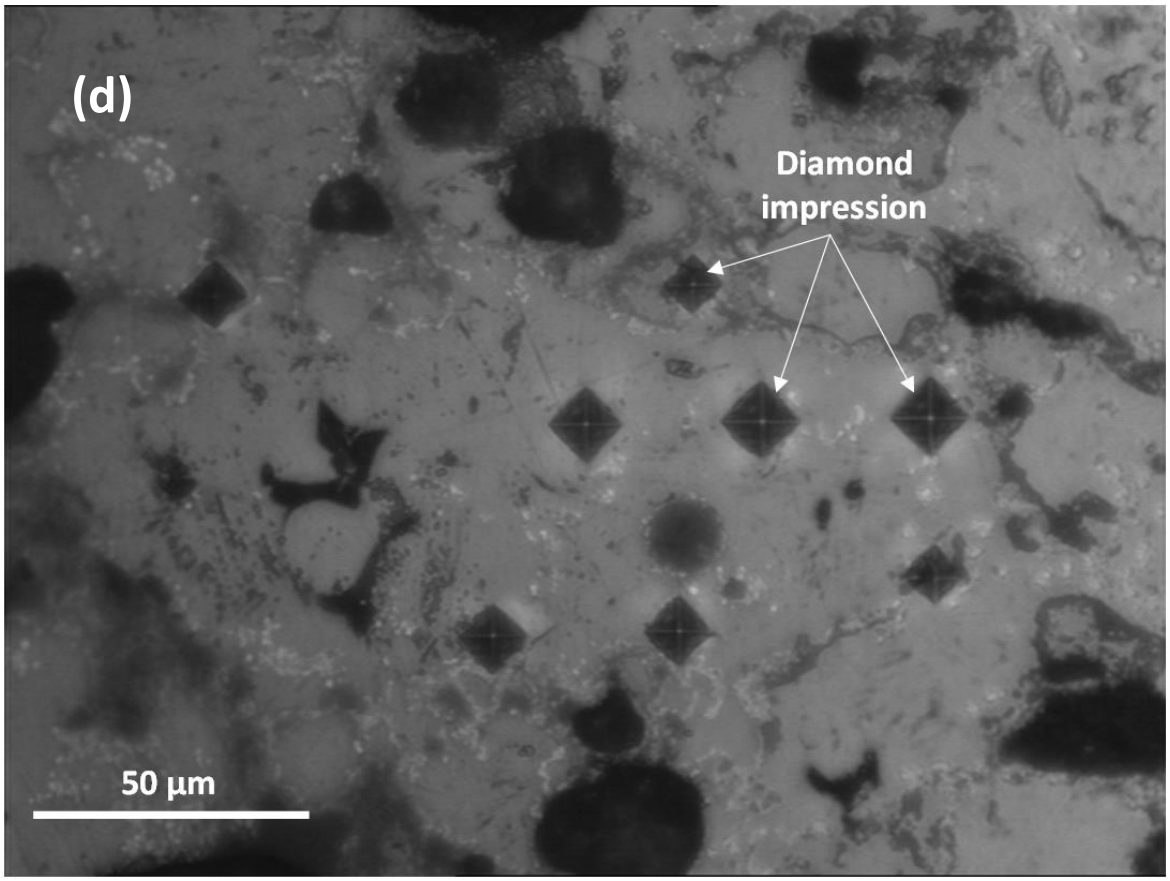
(d)
Diamond
impression
50 µm

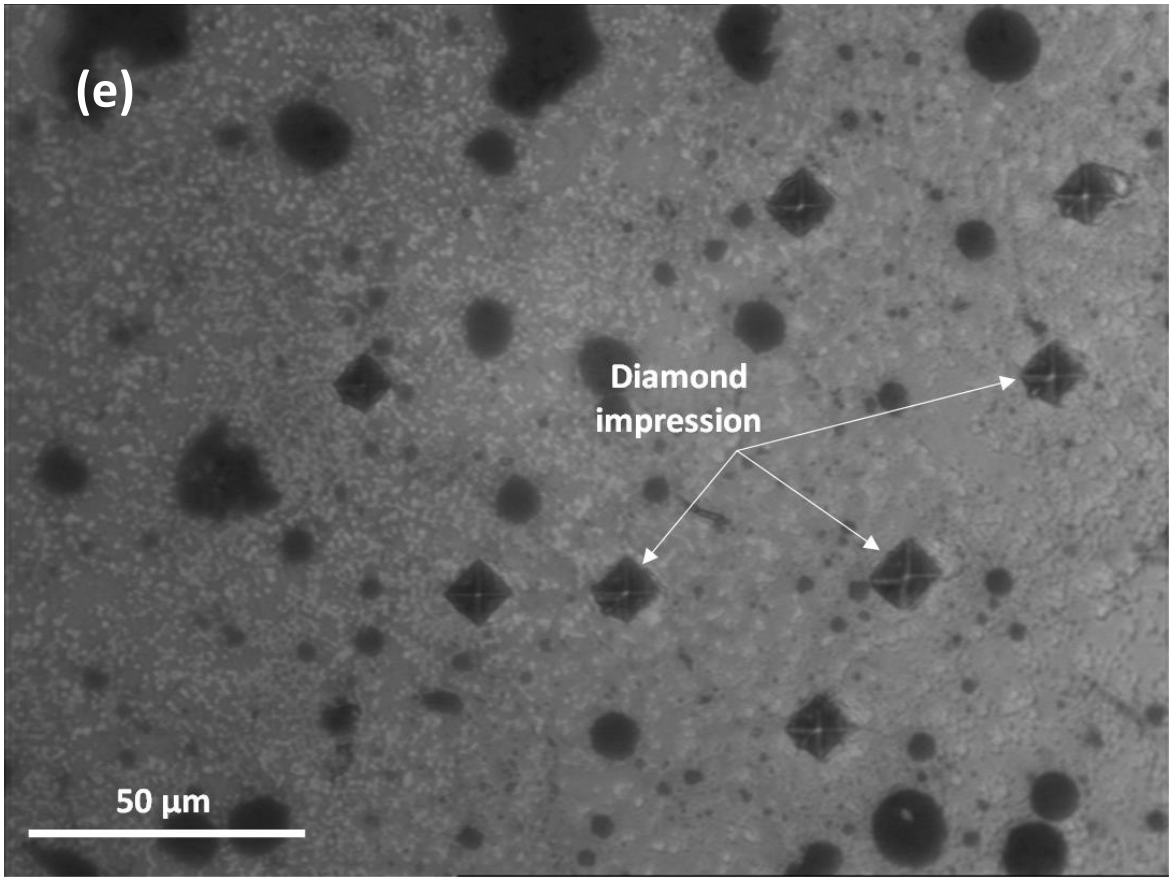
(e)
Diamond
impression
50 µm

Fig. 6 Impressions of Vickers indentation in the samples with (a) 0, (b) 10, (c) 20, (d) 30 and (e) 40 wt. %TiO_2/Al/C

4. Discussion

The temperature profilesof Ni/Al and TiO_2/Al/C reactions are essential to study the reaction mechanism of the systems. Although the reactants were prepared with a stoichiometric ratio of Ni/Al and $3TiO_2$/4Al/3C with different weight percentages, they were subsequently mixed together into Ni–Al–TiO_2–C systems. However, when the reactions are complete it is reasonable to assume that the synthesized products will be composed of NiAl, TiC, and Al_2O_3 with different weight ratios. As described in Eq. (1) and Eq. (2), during the synthesis reaction of Ni–Al–TiO_2–C systems, it is assumed that two reactions will occur: Ni + Al → NiAl and $3TiO_2$ + 4Al + 3C → $2Al_2O_3$ + 3TiC. The reaction in the Ni–Al–TiO_2–C systems may occur firstly by an increase in the temperature of the sample due to the heat supplied by induction heating. Al is melted first as it has the lowest melting point compared to the other reactants (Tmelt Al = 934 K, Tmelt Ni = 1728 K) [31].The molten Al then encircles the Ni, C and TiO_2 particles. Following the melting of the aluminium, it is initially more favourable for the exothermic reaction of Ni/Al to occur. This is due to the ignition of Ni/Al reaction which can be initiated at or below the melting point of Al [31][32]. In addition, Ni atoms are easier to preheat using induction heating due their high magnetic permeability compared to C and TiO_2. As suggested by Ping Zhu et al. [31], there are three stages which occur in the combustion reaction of Ni/Al systems. The first stage is initiated after a third of the aluminium is melted. The temperature will increase from the melting point of Al to the decomposition of the intermediate phase $NiAl_3$ at 854 °C (1127 K). In this period, the reaction mechanism is the dissolution of solid Ni in the liquid Al. Other intermediate phases such as Ni_2Al_3 and Ni_5Al_3 can also be formed at this stage. In the second stage, the reaction is still the dissolution of Ni in the liquid Al which occurs from 854 °C to 1300 °C (1573 K). The third stage is dominated by the exothermic reaction of Ni/Al. In this stage, the reaction rate is very high and the temperature increases sharply to achieve its maximum value. After the Ni/Al reaction is complete, the heat released by the formation of NiAl becomes the ignition agent to initiate further reactions in the TiO_2/Al/C system to form TiC–Al_2O_3 phases. According to Moore et al. [21] and Sharifi et al. [38], the SHS process of TiO_2/Al/C systems involves two reactions: the metallothermic reduction of the oxide (TiO_2) to form an elemental Ti, and the reaction between Ti and C to form TiC. These reactions are described in equations. (3) and (4). These are known

as thermite reactions as they are strongly exothermic and spontaneous. The heat of formation (ΔH_f) for different systems is given in

Table 3, where the negative signs indicate that the reactions are exothermic. Since the combustion temperature of a TiO_2/Al/C reaction is sufficiently high, the heat released by TiC–Al_2O_3 reactions can then maintain the synthesized NiAl in the liquid form causing TiC particles to insert into the NiAl melt [3]. The addition of TiC and Al_2O_3 contents into the NiAl increases the combustion exothermicity of the systems. As given in Table 3, the reaction of TiC + Al_2O_3 (ΔH = -1074.7 kJ/mol, Tad = 2325 K) is approximately nine times greater than the enthalpy reaction of NiAl (ΔH = -118.4 kJ/mol, Tad = 1912 K). The thermodynamic calculation of adiabatic temperature is given in

Reactions	ΔH_f (kJ/mol)	Ref.
Ni + Al → NiAl	-118.4	[34]
$4Al + 3TiO_2 \rightarrow 2Al_2O_3 + 3Ti$	-521.2	[38]
Ti + C → TiC	-184.5	[34]
$3TiO_2 + 4Al + 3C \rightarrow 3TiC + 2Al_2O_3$	-1074.7	[38]

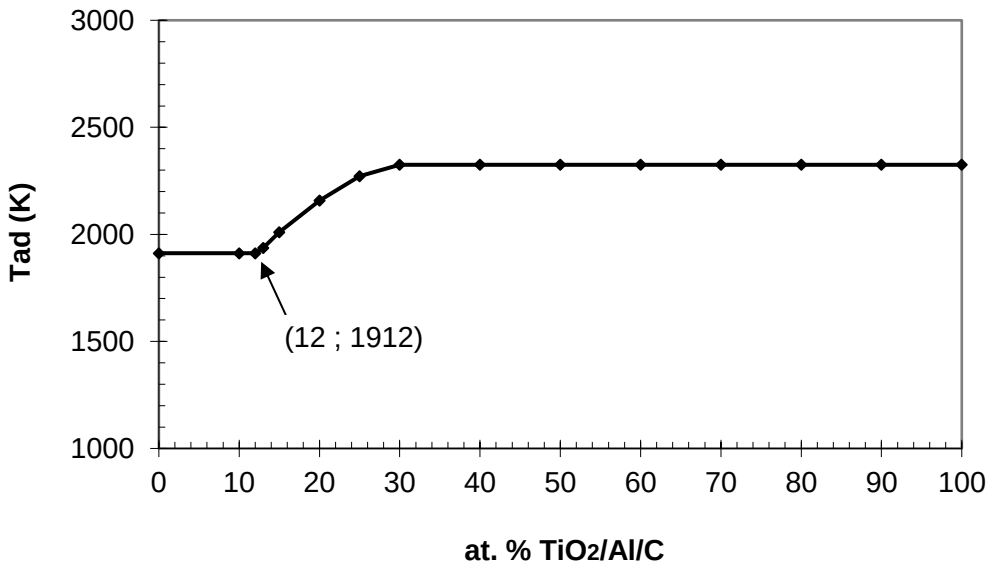

Fig. 7. An increased content of TiO_2/Al/C increases the adiabatic temperature of the systems starting from 12 at.% of TiO_2/Al/C. The adiabatic temperature will level off at 2325 K as the melting point of Al_2O_3. The addition of TiO_2/Al/C content in the range of 12 and 30 at.% with the reduced content of NiAl can then strengthen the exothermicity of the reaction, which is in accordance with that as obtained by Yeh et al. [13].

$$4Al + 3TiO_2 \rightarrow 2Al_2O_3 + 3Ti \quad (3)$$

$$Ti + C \rightarrow TiC \quad (4)$$

Table 3 Heat of formation at 298 K for different systems

Reactions	ΔH_f (kJ/mol)	Ref.
$Ni + Al \rightarrow NiAl$	-118.4	[34]
$4Al + 3TiO_2 \rightarrow 2Al_2O_3 + 3Ti$	-521.2	[38]
$Ti + C \rightarrow TiC$	-184.5	[34]
$3TiO_2 + 4Al + 3C \rightarrow 3TiC + 2Al_2O_3$	-1074.7	[38]

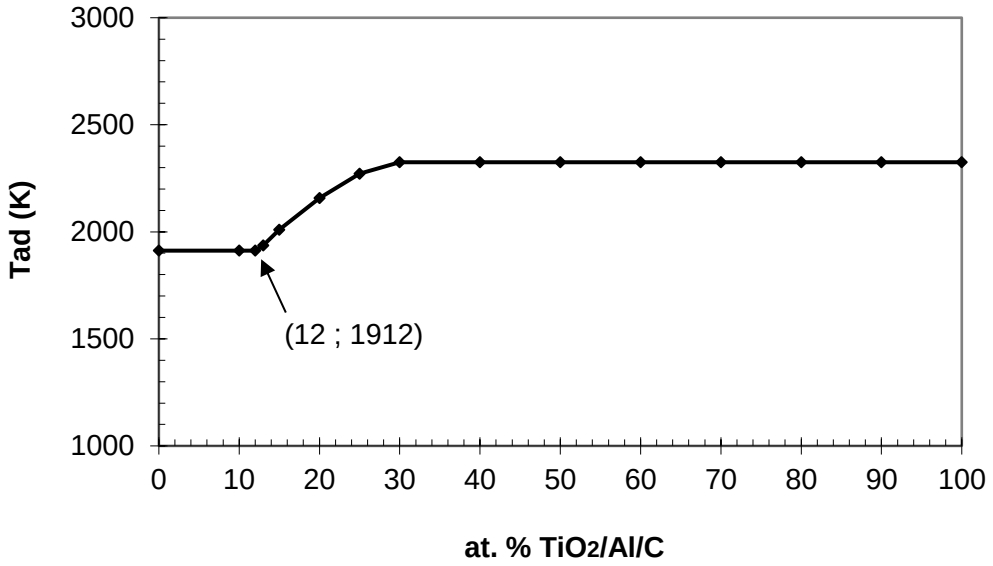

Fig. 7 Effect of TiO_2/Al/C additions on adiabatic temperature of NiAl/Al_2O_3/TiC reactions

5. Conclusions

The self-propagation high-temperature synthesis (SHS) process was successfully used to produce NiAl–TiC–Al_2O_3 composites using Ni/Al with TiO_2/Al/C as additives. The profile of the combustion temperature demonstrates that two stages of reactions exist in the SHS process, corresponding to the exothermic reaction of NiAl followed by TiO_2/Al/C system and the formation of NiAl and TiC–Al_2O_3. The addition of TiO_2/Al/C contents into Ni/Al increases the combustion exothermicity of the systems which increased the maximum reaction temperature. As the content of TiO_2/Al/C increases, the porosity of the synthesized product is increased since their resulting products, TiC and Al_2O_3 particles remain as solids during the process. However, the higher content of the TiC and Al_2O_3 in the composite system improves the hardness of the synthesized product. Increasing the TiO_2/Al/C content from 10 to 30 wt.% affects the shapes and distribution of Al_2O_3 and TiC. The synthesized Al_2O_3 changes from fine cluster to needle like shaped particles distributed along the boundary of the NiAl matrix. The size of the TiC particles increases from about 1-2 μm to 2-3 μm due to its nucleation and growth after the reaction.

Acknowledgement

This work was performed jointly in Kingston University London, UK and Universitas Muhammadiyah Surakarta, Indonesia. Part of the work was also conducted at London South Bank University, UK (Vickers microhardness test) and Wuhan University of Technology, PR China (XRD test). The authors would like to thank all contributions given to this work, which was financially supported by the Directorate General of Research and Development Strengthening, Ministry of Research, Technology and Higher Education of the Republic of Indonesia [Grant No. 72.94/A.3-III/LPPM/III/2018].

References

[1] N. S. Stolo, C. T. Liu, and S. C. Deevi, “Emerging applications of intermetallics,” *Intermetallics*, vol. 8, pp. 1313–1320, 2000. https://doi.org/10.1016/S0966-9795(00)00077-7

[2] Y. Zhang, S. Ji, and Z. Fan, “Improvement of mechanical properties of Al-Si alloy with effective grain refinement by in-situ integrated Al2.2Ti1B-Mg refiner,” *J. Alloys Compd.*, vol. 710, pp. 166–171, 2017.https://doi.org/10.1016/j.jallcom.2017.03.244

[3] X. Zhu, T. Zhang, D. Marchant, and V. Morris, “Combustion synthesis of TiC–NiAl composite by induction heating,” *J. Eur. Ceram. Soc.*, vol. 30, no. 13, pp. 2781–2790, Oct. 2010.https://doi.org/10.1016/j.jeurceramsoc.2010.06.002

[4] S. Hou, Z. Liu, and D. Liu, “The study of NiAl–TiB_2 coatings prepared by electro-thermal explosion ultrahigh speed spraying technology,” *Surf. Coat. Technol.*, vol. 205, no. 19, pp. 4562–4568, 2011.https://doi.org/10.1016/j.surfcoat.2011.03.122

[5] G. Gottstein, K. Reichert, K. Wen, R. Cremer, W. Hu, and D. Neuschu, “Influence of BN fiber coatings on the interfacial structure of sapphire fiber reinforced NiAl composites,” *Appl. Surf. Sci.*, vol. 179, pp. 150–155, 2001. https://doi.org/10.1016/S0169-4332(01)00255-0

[6] X. Zhu, T. Zhang, V. Morris, and D. Marchant, “Combustion synthesis of NiAl/Al_2O_3 composites by induction heating,” *Intermetallics*, vol. 18, no. 6, pp. 1197–1204, Jun. 2010. https://doi.org/10.1016/j.intermet.2010.03.009

[7] K. Cho, K. Ikeda, and H. Y. Yasuda, “Improvement of room and high temperature tensile properties of NiAl-strengthened ferritic heat-resistant steels through Mo addition,” *Mater. Sci. Eng. A*, vol. 728, pp. 239–250, 2018. https://doi.org/10.1016/j.msea.2018.05.034

[8] M. Beyhaghi, J. Vahdati Khaki, M. Manawan, A. Kiani-Rashid, M. Kashefi, and S. Jonsson, “In-situ synthesis and characterization of nano-structured NiAl-Al_2O_3 composite during high energy ball milling,” *Powder Technol.*, vol. 329, pp. 95–106, 2018. https://doi.org/10.1016/j.powtec.2018.01.052

[9] H. Zhang, H. Zhu, J. Huang, J. Li, and Z. Xie, “In-situ TiB_2-NiAl composites synthesized by arc melting: Chemical reaction, microstructure and mechanical strength,” *Mater. Sci. Eng. A*, vol. 719, pp. 140–146, 2018.https://doi.org/10.1016/j.msea.2018.01.125

[10] H. Z. Cui, L. Ma, L. L. Cao, F. L. Teng, and N. Cui, “Effect of NiAl content on phases and microstructures of TiC-TiB_2-NiAl composites fabricated by reaction synthesis,” *Trans. Nonferrous Met. Soc. China (English Ed.)*, vol. 24, no. 2, pp. 346–353, 2014. https://doi.org/10.1016/S1003-6326(14)63067-3

[11] X. jie Song, H. zhi Cui, L. li Cao, and P. Y. Gulyaev, “Microstructure and evolution of (TiB_2+Al_2O_3)/NiAl composites prepared by self-propagation high-temperature synthesis,” *Trans. Nonferrous Met. Soc. China (English Ed.)*, vol. 26, no. 7, pp. 1878–1884, 2016. https://doi.org/10.1016/S1003-6326(16)64265-6

[12] J. Yuan, X. Zhang, B. Li, X. Wang, and K. Sun, “Microstructure and tribological behavior of NiAl/WC composites fabricated by thermal explosion reaction at 800 °C,” *J. Alloys Compd.*, vol. 693, no. 17923, pp. 70–75, 2017. https://doi.org/10.1016/j.jallcom.2016.09.022

[13] C. L. Yeh, C. Y. Ke, and Y. C. Chen, “In situ formation of TiB_2/TiC and TiB_2/TiN reinforced NiAl by self-propagating combustion synthesis,” *Vacuum*, vol. 151, pp. 185–188, 2018.https://doi.org/10.1016/j.vacuum.2018.02.024

[14] W. Hu *et al.*, “Microstructural characterization and mechanical properties of a novel TiC-based cermet bonded with Ni_3(Al,Ti) and NiAl duplexalloy,” *Mater. Charact.*, vol. 135, no.

November 2017, pp. 295–302, 2018.
https://doi.org/10.1016/j.matchar.2017.11.003

[15] D. Vallauri and I. C. At, "TiC–TiB_2 composites: A review of phase relationships, processing and properties," *J. Eur. Ceram. Soc.*, vol. 28, pp. 1697–1713, 2008.
https://doi.org/10.1016/j.jeurceramsoc.2007.11.011

[16] X. Q. You, T. Z. Si, N. Liu, P. P. Ren, Y. D. Xu, and J. P. Feng, "Effect of grain size on thermal shock resistance of Al_2O_3–TiC ceramics," *Ceram. Int.*, vol. 31, no. 1, pp. 33–38, Jan. 2005.https://doi.org/10.1016/j.ceramint.2004.02.009

[17] L. Y. Y. Sheng, F. Yang, J. T. T. Guo, T. F. F. Xi, and H. Q. Q. Ye, "Investigation on NiAl–TiC–Al_2O_3 composite prepared by self-propagation high temperature synthesis with hot extrusion," *Compos. Part B Eng.*, vol. 45, no. 1, pp. 785–791, Feb. 2013.
https://doi.org/10.1016/j.compositesb.2012.05.038

[18] P. Mossino, "Some aspects in self-propagating high-temperature synthesis," *Ceram. Int.*, vol. 30, no. 3, pp. 311–332, Jan. 2004.https://doi.org/10.1016/S0272-8842(03)00119-6

[19] J. J. Moore and H. J. Feng, "Combustion synthesis of advanced materials: Part I. Reaction parameters," *Prog. Mater. Sci.*, vol. 39, no. 4–5, pp. 243–273, Jan. 1995.
https://doi.org/10.1016/0079-6425(94)00011-5

[20] K. Morsi, "Review: reaction synthesis processing of Ni–Al intermetallic materials," *Mater. Sci. Eng. A*, vol. 299, no. 1–2, pp. 1–15, Feb. 2001.
https://doi.org/10.1016/S0921-5093(00)01407-6

[21] J. J. Moore and H. J. Feng, "Combustion Synthesis of Advanced Materials: Part II. Classification, Applications and Modelling," *Prog. Mater. Sci.*, vol. 39, pp. 275–316, 1995.
https://doi.org/10.1016/0079-6425(94)00012-3

[22] A. Bansiddhi, T. D. Sargeant, S. I. Stupp, and D. C. Dunand, "Porous NiTi for bone

implants: A review," *Acta Biomater.*, vol. 4, pp. 773–782, 2008. https://doi.org/10.1016/j.actbio.2008.02.009

[23] H. X. Peng, Z. Fan, and J. R. G. Evans, "Bi-continuous metal matrix composites," *Mater. Sci. Eng. A*, vol. 303, no. 1–2, pp. 37–45, 2001. https://doi.org/10.1016/S0921-5093(00)01879-7

[24] P. Z. Shen *et al.*, "Development of a new graded-porosity FeAl alloy by elemental reactive synthesis," *Desalination*, vol. 249, no. 1, pp. 29–33, 2009. https://doi.org/10.1016/j.desal.2009.06.012

[25] Z. Zhang *et al.*, "Direct continuous hydrothermal synthesis of high surface area nanosized titania," *J. Alloys Compd.*, vol. 476, no. 1–2, pp. 451–456, 2009. https://doi.org/10.1016/j.jallcom.2008.09.036

[26] X. Wu *et al.*, "Novel Preparation, Microstructure, and Properties of Polyacrylonitrile-Based Carbon Nano fiber − Graphene Nanoplatelet Materials," *ACS Omega*, vol. 1 (2), no. August, pp. 202–211, 2016.https://doi.org/10.1021/acsomega.6b00063

[27] X. Zhang, F. Song, Z. Wei, W. Yang, and Z. Dai, "Microstructural and mechanical characterization of in-situ TiC/Ti titanium matrix composites fabricated by graphene/Ti sintering reaction," *Mater. Sci. Eng. A*, vol. 705, no. 29 September 2017, pp. 153–159, 2017. https://doi.org/10.1016/j.msea.2017.08.079

[28] T. W. B. Riyadi, T. Zhang, D. Marchant, and X. Zhu, "Synthesis and fabrication of NiAl coatings with Ti underlayer using induction heating," *Surf. Coatings Technol.*, vol. 258, pp. 154–159, 2014.https://doi.org/10.1016/j.surfcoat.2014.09.037

[29] X. Zhu, T. Zhang, D. Marchant, and V. Morris, "The structure and properties of NiAl formed by SHS using induction heating," *Mater. Sci. Eng. A*, vol. 528, no. 3, pp. 1251–1260, Jan. 2011.https://doi.org/10.1016/j.msea.2010.10.002

[30] L. H. S. R. Rahbari G, M. Hamdi, and and R. Yahya, “Combustion synthesis of TiO_2-Al-C/Al_2O_3 mixture in the presence of oxygen,” *J. Phys. Conf. Ser.*, vol. 152, no. 12055, pp. 1–9, 2009.https://doi.org/10.1088/1742-6596/152/1/012055

[31] P. Zhu, J. C. . Li, and C. Liu, “Reaction mechanism of combustion synthesis of NiAl,” *Mater. Sci. Eng. A*, vol. 329–331, pp. 57–68, Jun. 2002. https://doi.org/10.1016/S0921-5093(01)01549-0

[32] A. Makino, D. Ichikawa, A. Matsumoto, T. Kanda, and T. Watanabe, “Spontaneous ignition temperature for the compacted mixture of Ni–Al system: Experiment, theory, and comparisons,” *Proc. Combust. Inst.*, vol. 34, no. 2, pp. 2197–2204, Jan. 2013. https://doi.org/10.1016/j.proci.2012.07.002

[33] M. Ali-Rachedi, W. Ramdane, D. Vrel, A. Benaldjia, P. Langlois, and M. Guerioune, “The role of sintering additives on synthesis of cermets by auto-combustion,” *Powder Technol.*, vol. 197, no. 3, pp. 303–308, Jan. 2010. https://doi.org/10.1016/j.powtec.2009.10.009

[34] O. Kubaschewsky, *Materials Thermochemistry*, 6th ed. Pergamon Press, 1993.

[35] W. Xi, H. Wang, J. Li, and C. Shi, “A NiAl- and TiC-reinforced Fe-based nanocomposite prepared by the rapid-solidification thermite process,” *Mater. Sci. Eng. A*, vol. 541, pp. 166–171, Apr. 2012.https://doi.org/10.1016/j.msea.2012.01.132

[36] J. Guo *et al.*, “Wear properties of NiAl based materials,” *Prog. Nat. Sci. Mater. Int.*, vol. 22, no. 5, pp. 414–425, Oct. 2012.https://doi.org/10.1016/j.pnsc.2012.10.008

[37] Q. Dong, Q. Tang, and W. Li, “Al_2O_3–TiC–ZrO_2 nanocomposites fabricated by combustion synthesis followed by hot pressing,” *Mater. Sci. Eng. A*, vol. 475, no. 1–2, pp. 68–75, Feb. 2008.https://doi.org/10.1016/j.msea.2007.01.158

[38] E. Mohammad Sharifi, F. Karimzadeh, and M. H. Enayati, “Mechanochemically

synthesized Al_2O_3–TiC nanocomposite," *J. Alloys Compd.*, vol. 491, no. 1–2, pp. 411–415, Feb. 2010.https://doi.org/10.1016/j.jallcom.2009.10.206